Fluid Phase Equilibria 476 (2018) 30–38

Contents lists available at ScienceDirect

Fluid Phase Equilibria

journal homepage: www.elsevier.com/locate/fluid

Predictions of water/oil interfacial tension at elevated temperatures and pressures: A molecular dynamics simulation study with biomolecular force fields

Konstantinos D. Papavasileiou [a], Othonas A. Moultos [b], Ioannis G. Economou [a, c, *]

[a] National Center for Scientific Research "Demokritos", Institute of Nanoscience and Nanotechnology, Molecular Thermodynamics and Modelling of Materials Laboratory, GR-15310 Aghia Paraskevi Attikis, Greece
[b] Engineering Thermodynamics, Process & Energy Department, Faculty of Mechanical, Maritime and Materials Engineering, Delft University of Technology, Leeghwaterstraat 39, 2628CB Delft, The Netherlands
[c] Texas A&M University at Qatar, Chemical Engineering Program, Education City, PO Box 23874, Doha, Qatar

ARTICLE INFO

Article history:
Received 6 April 2017
Received in revised form
29 April 2017
Accepted 4 May 2017
Available online 8 May 2017

Keywords:
Interfacial tension
Toluene
n-dodecane
Molecular dynamics simulations

ABSTRACT

The interfacial properties of water/oil mixtures is a topic of significant interest for the oil and gas and chemical industry, as they are required for performing process calculations. However, the reported data at high temperatures and pressures are scarce. The present study focuses on simulating the interfacial tension (IFT) of mixtures of water with i) toluene (water/toluene), ii) *n*-dodecane (water/*n*-dodecane) and iii) a 50:50 % wt toluene:*n*-dodecane mixture (water/toluene/*n*-dodecane), at 1.83 MPa and temperatures ranging from 383.15 to 443.15 K. Molecular Dynamics (MD) simulations with atomistic molecular models, developed primarily for biomolecular systems were employed. In the simulations performed, the effects of the water model and the scaling of interatomic interactions by introducing a binary interaction parameter, k_{ij}, were assessed for the accurate reproduction of experimental data. The combination of the TIP4P/2005, SPC/E and TIP3P water models with the GAFF and Lipid14 force fields for toluene and *n*-dodecane respectively, coupled with appropriate binary interaction parameters, k_{ij}, for the interaction of carbon with oxygen atoms were found to yield accurate results in the case of binary mixtures. For the water/toluene/*n*-dodecane mixture, all force field combinations tested resulted in overestimated IFT values for the whole range of state points examined. Our simulations show that these widely used force fields, originating from the world of biomolecular simulations, are suitable candidates in the study of binary water/oil mixtures. Nevertheless, the introduction of the k_{ij} scaling parameter is not sufficient to allow the accurate reproduction of experimental IFT data for ternary water/oil/oil mixtures.

1. Introduction

The 9th Industrial Fluid Properties Simulation Collective Challenge [1] aimed at testing the ability of molecular modeling approaches to predict water/oil interfacial tension (IFT) at elevated temperatures and pressures for three different oils/water mixtures, namely water with toluene, *n*-dodecane and a 50:50 % wt mixture of *n*-dodecane and toluene. The IFT, γ, of water/oil systems is one of the basic physical properties required for performing process design calculations in oil and gas and chemical industry [2]. IFT is defined as the force per unit length that is required to increase the surface area between two immiscible fluids in contact [3]. It is an essential property for the description of liquid-liquid interfaces, as it controls contact phase hydrodynamics and mass transfer [4]. Experimentally, IFT is measured by a variety of methods, such as the spinning drop, the du Noüy ring, the Wilhelmy plate etc. [5,6]. Previous IFT studies on binary water/*n*-alkane [7–9], water/toluene [8,10,11] and ternary mixtures of water/*n*-alkane/toluene [12] referred to ambient conditions. However, at high temperatures and pressures only a few data have been reported [4,7,13–18]. Typically, these conditions involve temperatures that reach and exceed 370 K, while pressures applied are normally beyond 0.1 MPa in order to maintain the liquid state. A common thread in these

* Corresponding author. Texas A&M University at Qatar, Chemical Engineering Program, Education City, PO Box 23874, Doha, Qatar.
E-mail address: ioannis.economou@qatar.tamu.edu (I.G. Economou).

http://dx.doi.org/10.1016/j.fluid.2017.05.004
0378-3812/

studies is the IFT tendency to decrease with increasing temperature at constant pressure. Pressure effects are shown to be less pronounced [7], with IFT increasing with increasing pressure at constant temperature [7,19–21].

Several simulation studies have been dedicated to the examination of the IFT water/oil mixtures. These include application of Monte Carlo (MC) [22,23], Molecular Dynamics (MD) [24–28] and mesoscale modelling techniques such as Dissipative Particle Dynamics (DPD) [29] and Coarse-Grained Molecular Dynamics (CGMD) [30,31]. CGMD methods have been enriched recently with force fields developed with the SAFT-γ Mie equation of state (eos) top-down approach, which has been successfully applied in MD simulations for the prediction of several water/oil mixture properties [32]. Within the framework of this challenge, we calculated the IFT of these mixtures by means of interfacial MD simulations, a robust and reliable simulation technique in the study of water/oil systems.

The accuracy of the molecular models, describing the intra- and inter-molecular interactions, employed in simulations are of outmost importance for attaining accurate IFT values [33]. To this extend, our attempts focused on incorporating and benchmarking the performance of well-established atomistic molecular models coming from the world of biomolecular simulations in systems of interest to the chemical/petrochemical industry. More specifically, for the description of the organic phase we employed the General AMBER force field (GAFF) [34] and the Lipid14 [35] force field for toluene and *n*-dodecane, respectively. GAFF was developed for the incorporation of small organic molecules to existing AMBER force fields for proteins and nucleic acids. In early attempts of lipid simulations for a range of phospholipid bilayers GAFF showed great potential in the reproduction of experimental membrane properties, such as the area per lipid, the area compressibility modulus, lipid order parameters and others [36,37]. However, reoccurring issues at long timescales and constant pressure such as a liquid-to-gel phase transition above the phase transition temperatures were observed [38–40]. Similar issues were observed also for the OPLS-AA force field for *n*-alkanes longer than *n*-hexane, thus prompting for the development of the L-OPLS force field [41], which was parametrized in order to accurately reproduce liquid densities and viscosities of long hydrocarbons [42]. Therefore, dedicated efforts to tackle these problems led to the development of a new family of lipid force fields based on GAFF, with Lipid14 being its latest variant. Lipid14 features optimized alkyl chain dihedral angle terms and Lennard-Jones (LJ) parameters, allowing for tensionless simulations of lipid systems. The key features of these models are their enhanced compatibility with and transferability to a wide range of physical systems, ranging from proteins, lipids to organic compounds [34,35,43].

No prior attempts to utilize the Lipid14 in calculations of non-biological systems have been reported in literature. Recently, Kumar et al. [44] evaluated GAFF's performance in the prediction of liquid–vapor saturation properties of naphthalene derivatives. GAFF exhibited high accuracy of the liquid–vapor saturation properties and thus was proved to be a reasonable choice for describing the phase behavior of systems relevant to the oil and gas industry. In addition, the computational benchmarking of 146 organic liquids by Caleman et al. [45] showed that GAFF performs well in the prediction of several properties such as density, enthalpy of vaporization, heat capacities, and others.

We therefore grasped the opportunity of this 9th Challenge in order to evaluate the performance of these models in systems of industrial interest, which briefly encapsulates the novelty of the present work. In addition, we have examined the effect of the non-bonded LJ interactions long-range treatment, the simulation duration and the impact of the choice of the water model on the calculated IFTs.

2. Simulation methods

2.1. Force fields

Toluene structure was initially optimized in the gas phase at the B3LYP/6-31G* level of theory [46–48], by means of the Gaussian 09 [49] suite of programs. Then, atomic charges were obtained from the optimized geometry at the HF/6-31G* level of theory according to the Mertz-Kollman population analysis scheme [50,51]. Consecutively, partial atomic charges were derived according to the RESP protocol [52], utilizing the ANTECHAMBER module [53] of the AMBER12 suite of programs [54]. GAFF parameters [34] were then assigned to toluene, the atom types of which are presented in Table S1 of the Supporting Information. Topologies were generated by means of the tLEaP module [54] and are illustrated in Table S2, along with the calculated partial charges.

n-dodecane was described by means of the Lipid14 force field parameters [35]. Partial charges for the *n*-dodecane chain were generated according to the original derivation procedure [35]. Specifically, fifty randomly selected *n*-dodecane molecules were extracted from the initial cubic box conformation and were subsequently used for the charge calculation. The Electrostatic Potential (ESP) [50,51] was calculated directly from each structure at the HF/6-31G* level of theory without optimization, and partial charges derived using the RESP fitting procedure [52] for each chain. Charges were then taken as an average over all fifty RESP fits. The structure and partial charges of *n*-dodecane are illustrated in Table S3 of the Supporting Information.

For the representation of water molecules the TIP4P/2005 [55], TIP3P [56] and SPC/E [57] models were employed. Our starting point was the TIP4P/2005 force field, which is a four-site rigid model with a LJ sphere fixed on the oxygen atom. The electrostatic contributions are implemented by positive partial charges assigned to the hydrogens and a negative partial charge on the additional site, located on the bisector of the H-O-H angle at a distance 0.1546 Å from the oxygen atom. The TIP4P/2005 model has been extensively tested and found to be very accurate for several water properties, including the vapor-liquid IFT [58–60]. On the other hand, the SPC/E and TIP3P force fields assume a single LJ site on the oxygen atom and three charges on oxygen and hydrogen atoms, respectively, while bond lengths and bond angles are kept fixed. The SPC/E force field, likewise to TIP4P/2005, is considered one of the best, two-body, non-polarizable, water models [61] and has also proved to be accurate in capturing the vapor-liquid IFT [59]. SPC/E does not use the experimental geometry of the water but instead two simple values for the bond length (1 Å) and angle (109.47°). The TIP3P is the most commonly used water model in biomolecular simulations [61] and it was primarily developed to reproduce its density and the vaporization enthalpy at ambient temperature and pressure conditions [56,61]. However, several studies have highlighted the TIP3P's poor performance in describing important water properties, thereby expressing serious concerns about its more generalized use [58,61]. Despite its known deficiencies, given that the Lipid14 and GAFF force fields have been parameterized for use primarily with the TIP3P water model [43] and that this combination is utilized in aqueous membrane bilayer simulations [36], this water model was also included in this study. The force field parameters of all the species involved are collected and presented in Tables S4 and S5 of the Supporting Information document.

Standard Lorentz–Berthelot combining rules [62] were used for the well depth ε and the size parameter σ to describe non-bonded LJ interactions between sites of different type *i* and *j* according to the

expressions:

$$\varepsilon_{ij} = \sqrt{\varepsilon_{ii}\varepsilon_{jj}} \text{ and } \sigma_{ij} = \frac{\sigma_{ii} + \sigma_{jj}}{2}. \quad (1)$$

The Berthelot (geometric mean) combining rule has been shown to work well for various properties of several binary mixtures of components, having atoms of similar sizes and ionization potentials [63–69]. However, it has been proven to be insufficient in the description of dispersion interactions between polar and non-polar components [63]. Previous simulation studies have shown that the combination of TraPPE *n*-alkanes and SPC/E water mixtures yields water solubilities that are underestimated by approximately an order of magnitude compared to their experimental values [70]. The source of this behavior may be primarily attributed to the inaccurate force field description of electrostatic and induction effects of water in *n*-alkane [71,72], as well as the crudely modeled water – *n*-alkane interactions based on the Lorentz – Berthelot combining rules. In order to attain better agreement with experiment, it has become customary to introduce corrections in terms of the deviation from the Berthelot rule [70], expressed as:

$$\varepsilon_{ij} = k_{ij}\sqrt{\varepsilon_{ii}\varepsilon_{jj}} \quad (2)$$

where, k_{ij} is a binary interaction parameter fitted to the experimental data. Such a parameter was also used in the present study, as it was previously found that the interfacial properties of the water/*n*-decane mixture were not sensitive to size parameter σ and the standard Lorentz combining rule was employed for the description of unlike sites [26].

2.2. Simulation details

The initial conformations of all systems were constructed by means of the Amorphous and Interface Builder modules integrated in Scienomics MAPS software package [73], according to which the constituent molecules were first inserted into the cubic boxes using a modified configuration bias scheme [74], which were later merged to produce final orthorhombic cells of the interfaces phases. The number of molecules used was 2000 for water and 250 for toluene and *n*-dodecane, respectively. In the ternary water/toluene/*n*-dodecane mixture, 162 toluene and 88 *n*-dodecane molecules were used, respectively, in order to properly account for the 50:50 (wt/wt) toluene/*n*-dodecane blend requirement of the challenge. Then, the generated GAFF, Lipid14 and TIP4P/2005, TIP3P and SPC/E topologies and coordinate files were converted to the GROMACS format by means of the ACPYPE utility [75] (Table S5). All topology and coordinate files are available as a Mendeley dataset [76].

The liquid-liquid IFT was obtained by interfacial MD simulations using GROMACS 5.0.7 software [77–81]. The simulations were performed in orthorhombic boxes, with periodic boundary conditions imposed in all directions (Fig. 1).

Prior to production runs and in order to eliminate any close contacts between atoms, all systems were subjected to steepest descent energy minimization for 20,000 steps. Then, short equilibration simulations in the canonical (*NVT*) and isobaric-isothermal-isointerface area (NP_NAT) ensembles were performed, where P_N is the input normal pressure and *A* the interfacial area. Specifically, all systems were gradually heated to the target temperatures for 100 ps in the *NVT* ensemble using the Berendsen thermostat [82], with the coupling constant set to 1 ps. LJ interactions were cut-off at 14 Å and the Particle Mesh Ewald (PME) method [83,84] was applied for the calculation of long-range electrostatic interactions at the same cut-off distance. The LINCS algorithm [85] restrained all bonds involving hydrogen atoms. The integration step of all simulations was set to 2 fs.

All systems were then equilibrated for a period of 5 ns in the NP_NAT ensemble, at constant pressure of 1.83 MPa using a Berendsen barostat [82] with the coupling constant set to 1 ps. Pressure coupling was isotropic in the x and y direction, but semi-isotropic in the z direction, which is perpendicular to the liquid-liquid interface. During this period, the density of both liquid phases converged to a mean value (Fig. 1), along with the energy of the system.

The IFT, γ, was evaluated by using the diagonal stress tensor elements (P_{xx}, P_{yy}, and P_{zz}) through the following expression [86–88]:

$$\gamma = \frac{1}{2}\left\langle L_z\left(P_{zz} - \frac{P_{xx} + P_{yy}}{2}\right)\right\rangle \quad (3)$$

where, L_z is the length of the simulation box in the z direction, normal to the water/oil interface which forms along the xy plane. The factor ½ is due to the presence of two interfaces and angle brackets represent the ensemble average.

For the purposes of the challenge, IFTs were calculated without employing any modifications to LJ combining rules from a single 5 ns run per state point, in the NP_NAT ensemble using the Nosé–Hoover thermostat [89], while maintaining the semi-isotropic pressure coupling with a Berendsen barostat [82]. IFT values and statistical uncertainties (95% confidence intervals) were obtained by dividing the production period of the simulations into five blocks (Table S6 of Supporting Information). After the submission to the challenge, longer production runs of 10 ns were performed. Each run was executed on 100 Intel Xeon E5-2680v2 cores and required approximately two wall-clock hours for completion. The simulation length was found to have no impact on IFT results (Table S7 of Supporting Information). It is important to note here, that the k_{ij} binary interaction parameter was fitted after the end of the challenge and upon disclosure of the experimental data.

The cut-off of the LJ interactions has a minor impact on the molecular arrangement, but significantly influences the computed values of properties such as the IFT. This is more profound in simulations of inhomogeneous systems, leading to incorrect estimation of interfacial properties [59]. Therefore, instead of using analytical tail corrections, we applied the Particle-mesh Ewald summation for the attractive LJ interactions (LJ-PME) [90]. This technique is computationally robust and has been successfully employed in the calculation of properties such as IFT [91]. However, previous works have shown that using LJ-PME with the GAFF force field, which has been optimized for a cut-off approach, leads to overestimated IFT for several organic liquids [92]. We investigated the effect of using the LJ-PME over the cut-off to the long-range LJ potential, using a radius of 16 Å a practice that has shown to be equally efficient [90]. Our IFT results showed no dependence on the long-range LJ treatment chosen (Table S7 of Supporting Information). Snapshots of the equilibrated structures of all systems are illustrated in Fig. 1.

3. Results and discussion

In this section, the MD simulations results for the series of water/oil mixtures investigated are presented. All IFT calculations are at the reference temperatures of 383.15, 403.15, 423.15 and 443.15 K and pressure of 1.83 MPa.

3.1. Berthelot combining rule

The density profiles illustrated in Fig. 1, show that the bulk region densities of water (TIP4P/2005) and *n*-dodecane (Lipid14) are

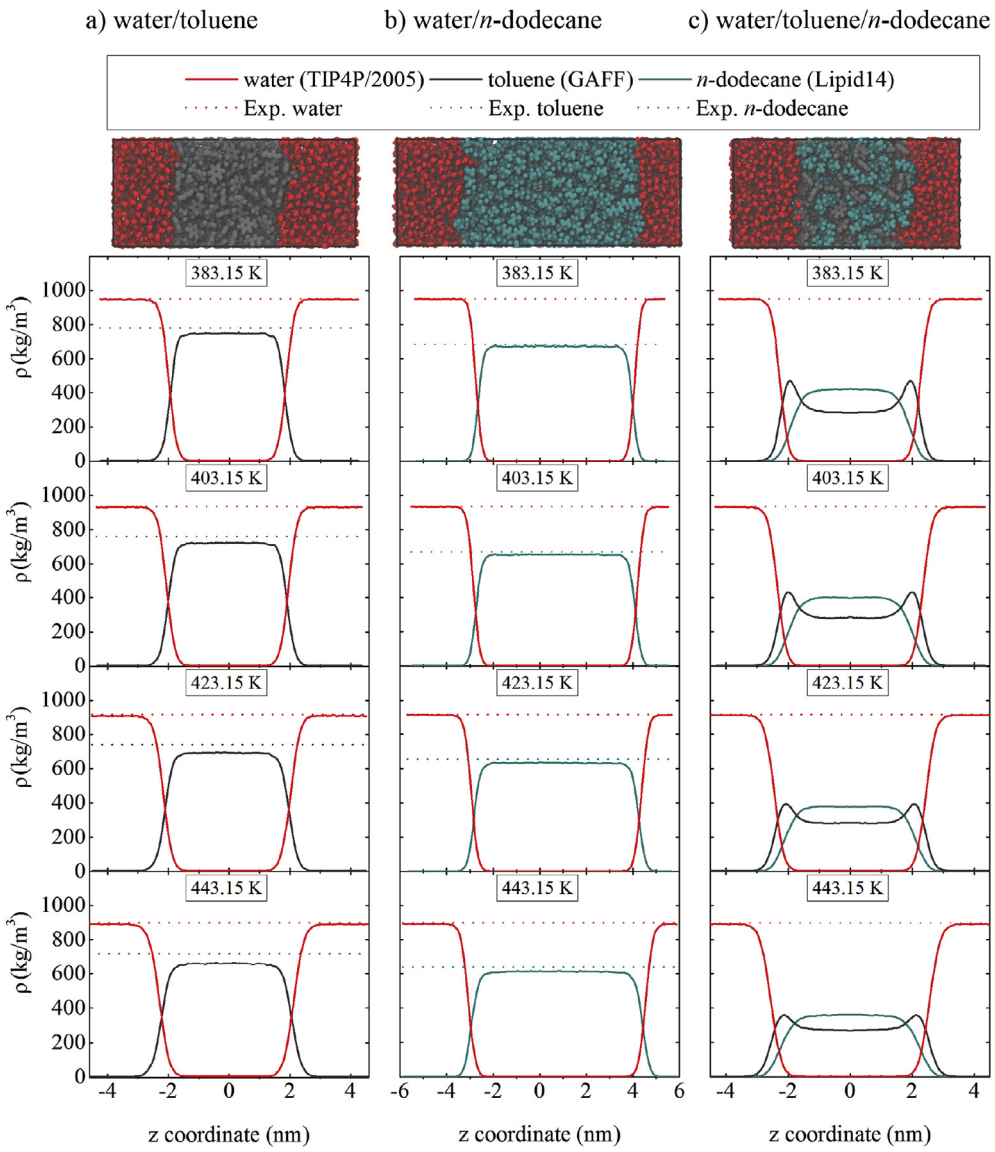

Fig. 1. Equilibrated structures and partial densities of all systems studied using the TIP4P/2005 water model, for various temperatures and pressure 1.83 MPa. Water, toluene and *n*-dodecane molecules are illustrated in red, gray and cyan colors, respectively. (For interpretation of the references to colour in this figure legend, the reader is referred to the web version of this article.)

close to their experimental values [93]. Toluene density is slightly underestimated by GAFF compared to its experimental value, a finding also reported by Caleman et al. at 298.15 K and 1 bar [45]. Furthermore, the density distribution of the water/toluene/*n*-dodecane mixture components is in agreement with previous simulation studies of water/oil interfaces, particularly with regard to the tendency of the toluene molecules to accumulate at the water interface (Fig. 1c) [28]. This accumulation phenomenon at water/oil interfaces is attributed to the weak hydrogen bonding between water and toluene at the interface [49]. These density distribution profiles are essentially the same for SPC/E, with the partial density being slightly underestimated compared to the experimental values at each temperature (Fig. S3 of Supporting Information). On the other hand, in the TIP3P water systems the underestimation of water density becomes more significant, a feature which should have an important effect on the accurate calculation of IFTs (Fig. S4).

From the results presented in Table 1, it is indicated that the IFT values in all systems and for all force fields studied decrease as temperature increases, reproducing the experimentally observed trends. Fig. 2 shows that there is an almost linear dependence between γ and T; this behavior is in agreement with previous experimental studies on water – *n*-alkane mixtures [13]. The water/*n*-dodecane mixture exhibits higher IFT compared to water/toluene, with the water/toluene/*n*-dodecane mixture adopting intermediate values.

These observations are in line with the experimental values used as a benchmark for the purposes of the challenge (Fig. 2). However, even though the combination of the GAFF and Lipid14 AMBER force fields with TIP4P/2005 appears to capture the correct trend, absolute IFT values are overestimated compared to the experimental ones by 20%, 27% and 30% on average for the water/toluene, water/*n*-dodecane and water/toluene/*n*-dodecane mixtures, respectively. The SPC/E displays the same behavior with TIP4P/2005. Furthermore, the overestimation is increasing with increasing temperature. It is also clear that the TIP3P water model

Table 1
Calculated IFT values for the various mixtures with the three different water models examined, without any scaling of the intermolecular interaction parameters (k_{ij}= 1).

T (K)	γ (mN/m)					
	water/toluene					
383.15	TIP4P/2005	33.1 ± 0.7	TIP3P	22.8 ± 0.3	SPC/E	31.1 ± 0.5	Experiment	28.6
403.15		31.2 ± 1.0		20.8 ± 0.6		29.4 ± 0.8		26.4
423.15		29.0 ± 0.6		18.8 ± 0.6		27.1 ± 0.7		23.8
443.15		25.9 ± 0.7		15.3 ± 0.6		24.8 ± 0.9		20.2
	water/*n*-dodecane					
383.15	TIP4P/2005	47.5 ± 0.8	TIP3P	36.8 ± 1.2	SPC/E	45.3 ± 1.2	Experiment	40.0
403.15		45.4 ± 0.8		33.4 ± 0.7		42.6 ± 0.7		36.5
423.15		42.4 ± 0.8		29.5 ± 0.6		39.9 ± 1.0		32.9
443.15		38.5 ± 1.1		26.1 ± 0.4		36.1 ± 0.9		28.5
	water/toluene/*n*-dodecane					
383.15	TIP4P/2005	38.7 ± 0.8	TIP3P	28.9 ± 0.6	SPC/E	37.5 ± 0.3	Experiment	31.4
403.15		36.4 ± 0.3		26.6 ± 1.1		35.3 ± 0.3		29.0
423.15		34.7 ± 0.4		23.6 ± 0.6		32.9 ± 0.5		26.1
443.15		31.6 ± 0.9		20.6 ± 0.4		29.0 ± 0.6		22.6

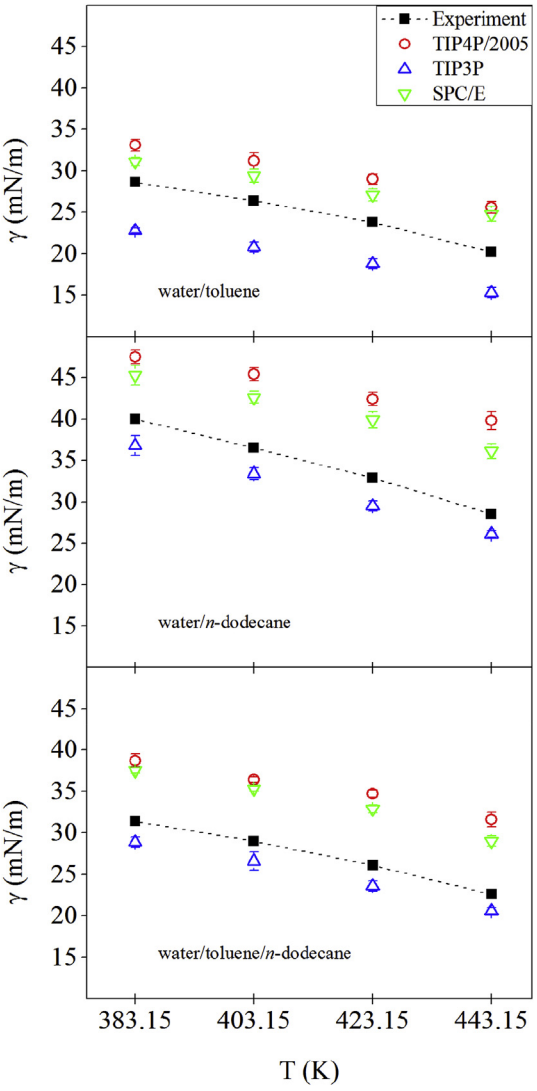

Fig. 2. Calculated IFT of water/toluene, water/*n*-dodecane and 50:50 (wt/wt) water/toluene/*n*-dodecane mixtures with the TIP5P/2005, TIP3P and SPC/E water models, without scaling of the intermolecular interaction parameters.

has a profound impact on IFT. Specifically, the IFT results of all mixtures are now underestimated but are slightly closer in absolute value compared to the experimental benchmark data. Furthermore, the TIP3P model leads to an improvement in the description of the IFT temperature dependence, especially in the case of the water/toluene mixture.

It is useful to note here that all water models have similar σ values for water oxygen, with differences in their ε values (Table S4 of the Supporting Information). In fact, the ε values decrease in the order $\varepsilon_{TIP4P/2005}>\varepsilon_{SPC/E}>\varepsilon_{TIP3P}$. Thus, by altering the ε_{ij} of the toluene and *n*-dodecane carbon and water oxygen atoms, respectively, one can fine-tune these models in order to achieve better agreement with the experimental IFT values.

3.2. Modified Berthelot combining rule

The simulations with scaled binary interaction parameters of the toluene and *n*-dodecane carbon and water oxygen atoms, respectively, resulted in better agreement with experiment. The k_{ij} values led to the most accurate results are presented in Table 2. One can observe that the TIP4P/2005 and SPC/E models were found to perform better with different k_{ij} for the aromatic and alkyl carbons with water oxygen. On the other hand, mixtures with the TIP3P model were in better agreement by setting a uniform k_{ij} = 0.8 value for all carbon atoms with water oxygen interactions. From the results listed in Table 3 and depicted in Fig. 3 become clear that the fine-tuning of the k_{ij} parameter can produce much improved water/oil IFT values. Nevertheless, upon closer examination, one can isolate subtle differences introduced to the simulations by the choice of water model.

The average absolute difference of simulated and experimental

Table 2
Binary interaction parameter values used for IFT predictions. The atom types refer to the interaction sites of toluene (ca: aromatic, c3: aliphatic) and *n*-dodecane (cD: aliphatic) carbons with water oxygen (OWT4: TIP4P/2005, OW: TIP3P and SPC/E oxygen types; for the actual force field parameters see Tables S1 and S4 of the Supporting Information).

Water model		toluene		*n*-dodecane
TIP4P/2005	Pair type	OWT4-c3	OWT4-ca	OWT4-cD
	Value	1.25	1.05	1.25
TIP3P	Pair type	OW-c3	OW-ca	OW-cD
	Value	0.80	0.80	0.80
SPC/E	Pair type	OW-c3	OW-ca	OW-cD
	Value	1.20	1.05	1.20

Table 3
Calculated IFT values with 95% confidence intervals using the three different water models, using parameters shown in Table 2.

T (K)	γ (mN/m)						
			water/toluene				
383.15	TIP4P/2005	28.1 ± 0.9	TIP3P	29.6 ± 0.9	SPC/E	28.4 ± 0.2	Experiment 28.6
403.15		26.2 ± 0.3		27.2 ± 0.4		26.5 ± 0.4	26.4
423.15		24.6 ± 0.6		23.6 ± 0.4		24.6 ± 0.7	23.8
443.15		22.7 ± 0.8		20.2 ± 0.5		22.1 ± 0.4	20.2
			water/*n*-dodecane				
383.15	TIP4P/2005	38.7 ± 1.2	TIP3P	39.8 ± 1.0	SPC/E	40.0 ± 1.3	Experiment 40.0
403.15		36.7 ± 0.8		36.2 ± 0.5		36.2 ± 0.7	36.5
423.15		33.7 ± 0.9		32.7 ± 0.3		33.6 ± 0.9	32.9
443.15		31.0 ± 0.8		28.4 ± 0.4		31.4 ± 1.1	28.5
			water/toluene/*n*-dodecane				
383.15	TIP4P/2005	32.6 ± 0.6	TIP3P	33.6 ± 0.5	SPC/E	33.2 ± 0.8	Experiment 31.4
403.15		30.5 ± 0.8		31.3 ± 0.6		30.8 ± 0.7	29.0
423.15		29.0 ± 0.9		27.4 ± 0.7		28.3 ± 0.5	26.1
443.15		27.2 ± 0.8		23.9 ± 0.6		25.9 ± 0.5	22.6

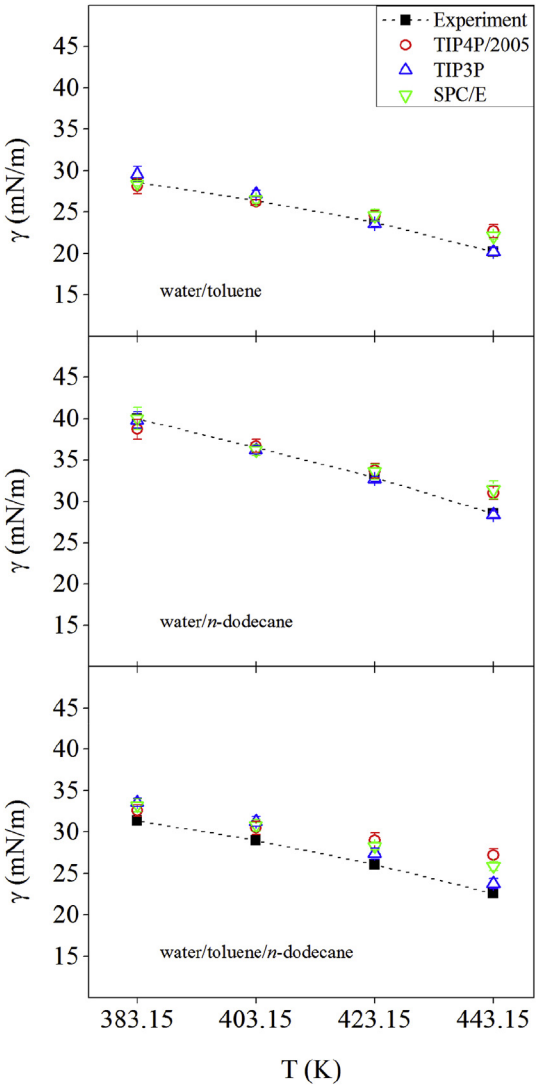

Fig. 3. Calculated IFT of water/toluene, water/*n*-dodecane and 50:50 (wt/wt) water/toluene/*n*-dodecane mixtures with the TIP5P/2005, TIP3P and SPC/E water models, by scaling the intermolecular carbon – oxygen interaction parameters. Binary interaction parameter values used for IFT predictions depending on the water model are provided in Table 2.

IFT values is ~2% for the water/toluene and water/*n*-dodecane mixtures for all water models used. This translates to an absolute difference of 1 mN/m. Despite the overall improvement, there seems to be a discrepancy that is not tackled even after the introduction of the k_{ij} parameter. More specifically, it is observed that the simulations including TIP4P/2005 and SPC/E systems show better agreement with experiments at lower temperatures, which is not followed at higher temperatures. This results in a different temperature dependence of IFT, which diverges from the experimental trend. The TIP3P model coupled with GAFF and Lipid14 for toluene and *n*-dodecane, respectively, results in better reproduction of the data for the entire temperature range examined. This can be attributed to the compatibility of the TIP3P model with the AMBER family of force fields.

Deviation from experiment becomes more pronounced in the case of the water/toluene/*n*-dodecane mixture. Calculated IFT values deviate by about 8%, which translates to approximately 3 mN/m on average for all systems. Similarly to the findings for the binary mixtures, the TIP4P/2005/GAFF/Lipid14 and SPC/E/GAFF/Lipid14 combinations result to IFTs that are closer to the experimental values at lower temperatures, while adopting slightly higher values compared to experiment as temperature increases (Table 3 and Fig. 3). The TIP3P/GAFF/Lipid14 combination shows the most consistent behavior, but IFT values are still overestimated by approximately 6%. This indicates that even though the simple k_{ij} scaling approach is adequate for improving results for the binary water/oil mixtures, it is not enough to capture the more complex intermolecular interactions in ternary water/oil/oil mixtures.

There appear to be significant differences in the interfacial loading of toluene depending on the water model used, which explains the differences in IFT. Given the different electrostatics of each water model, the attractive “weak hydrogen bonding” between the aromatic toluene and water molecules [28] is either enhanced (TIP4P/2005, SPC/E) or reduced (TIP3P). This explains the difference in toluene density observed with either water model (Fig. 4a). The preference of toluene to accumulate near the water interface in the water/toluene/*n*-dodecane mixture, not only explains the intermediate IFT values of the ternary compared to the binary mixtures, but also renders toluene loading at the interface as a controlling factor of the IFT.

From our simulations, it becomes clear that the use of the k_{ij} adjustable parameter alone is insufficient to predict accurately the experimental IFT data for ternary water/oil/oil mixtures. Fine-tuning the k_{ij} parameter results into a toluene density profile at

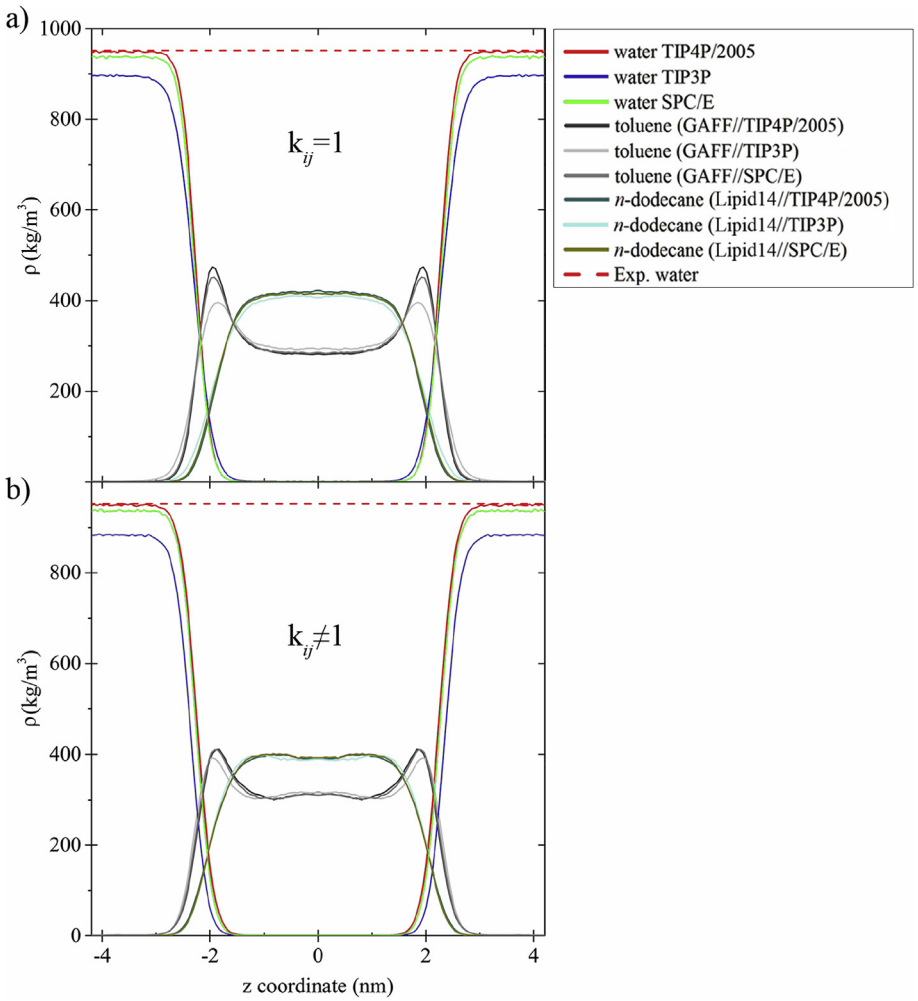

Fig. 4. Density profiles for the components of the ternary water/toluene/*n*-dodecane mixture at 383.15 K a) without and b) with scaling of the intermolecular carbon − oxygen interaction parameters (Table 2) for all force fields used.

the water/oil interface that is now common for all systems (Fig. 4b). This highlights the role of toluene as an active interfacial agent in the ternary mixture.

4. Conclusions

The present work entails extensive MD simulations of representative water/oil binary and ternary mixtures for the calculation of IFT. Our efforts concentrated primarily in incorporating atomistic force fields that have been primarily developed for biomolecular simulations in addressing industrially related properties like the IFT. The GAFF and Lipid14 force fields were employed for the description of toluene and *n*-dodecane, respectively. The partial density profiles of the oil phases were found to be in agreement with the respective experimental data. These molecular models were combined with three fixed-point-charge water models, namely the TIP4P/2005, TIP3P and SPC/E. The TIP3P model does not reproduce the experimental water density as accurately as its TIP4P/2005 and SPC/E counterparts do. Water model parameters are crucial in the prediction of IFT properties, as they are responsible for the significant overestimation (TIP4P/2005 and SPC/E) or the moderate underestimation (TIP3P) of IFT values compared to the experimental data.

Modifying the cross LJ interactions by appropriately adjusting the binary interaction parameter is a simple but effective way to improve the accuracy of the IFT predictions for binary mixtures. However, even by following this approach, the use of the TIP4P/2005 and SPC/E models leads to slightly overestimated IFT values at 443.15 K, weakly diverging from the experimental weak temperature IFT dependence. Surprisingly, the combination of the less accurate TIP3P water model with the aforementioned AMBER force fields, using a uniform $k_{ij} = 0.8$ parameter of the scaling of carbon-water oxygen interactions captures the overall IFT behavior more accurately compared to the other two water models. TIP3P's deficiency in accurately reproducing water density at the conditions examined is compensated by its compatibility with the AMBER force fields and aids towards calculation of IFTs that are in better agreement with experiment.

As far as the water/toluene/*n*-dodecane mixture is concerned, all simulations, regardless of the k_{ij} scaling used, led to overestimated IFT values compared to experimental findings. The TIP4P/2005 and SPC/E model behavior in higher temperatures pertains, while the TIP3P model shows better agreement. The overestimation of IFT for the ternary mixture cannot be compensated by the introduction of a simple k_{ij} binary parameter. The source of this discrepancy can be attributed to the initial atomistic force field parametrization of the pure components and to the actual combining rules used. Therefore, improved models that

include IFT data into their initial setup may lead to more accurate mixture calculations.

Author contributions

The manuscript was written through contributions of all authors. All authors have given approval to the final version of the manuscript.

Acknowledgments

This work was supported by computational time granted from the Greek Research & Technology Network (GRNET) (002043) in the National High Performance Computing facility - ARIS - under project ID002043. We are also thankful to the High Performance Computing center of Texas A&M University at Qatar for generous resource allocation. Scienomics SARL is acknowledged for providing MAPS software used to generate initial structures of the systems simulated.

Appendix A. Supplementary data

Supplementary data related to this article can be found at http://dx.doi.org/10.1016/j.fluid.2017.05.004.

References

[1] Industrial Fluid Properties Simulation Collective, http://fluidproperties.org, Accessed 14 March 2017.
[2] C.Y. Jian, M.R. Poopari, Q.X. Liu, N. Zerpa, H.B. Zeng, T. Tang, Reduction of water/oil interfacial tension by model asphaltenes: the governing role of surface concentration, J. Phys. Chem. B 120 (2016) 5646–5654.
[3] R.J. Hunter, L.R. White, Foundations of Colloid Science, Oxford University Press, Oxford Oxfordshire, 1987.
[4] T. Al-Sahhaf, A. Elkamel, A.S. Ahmed, A.R. Khan, The influence of temperature, pressure, salinity, and surfactant concentration on the interfacial tension of the n-octane-water system, Chem. Eng. Commun. 192 (2005) 667–684.
[5] A.W. Adamson, A.P. Gast, Physical Chemistry of Surfaces, sixth ed., Wiley, New York, 1997.
[6] J. Drelich, C. Fang, C.L. White, Measurement of interfacial tension in fluid-fluid systems, in: A. Hubbard (Ed.), Encyclopedia of Surface and Colloid Science, Marcel-Dekker, New York, 2002, pp. 3158–3163.
[7] B.Y. Cai, J.T. Yang, T.M. Guo, Interfacial tension of hydrocarbon plus water/brine systems under high pressure, J. Chem. Eng. Data 41 (1996) 493–496.
[8] N.R. Biswal, J.K. Singh, Interfacial behavior of nonionic Tween 20 surfactant at oil-water interfaces in the presence of different types of nanoparticles, RSC Adv. 6 (2016) 113307–113314.
[9] A. Goebel, K. Lunkenheimer, Interfacial tension of the water/*n*-alkane interface, Langmuir 13 (1997) 369–372.
[10] N.N. Dutta, G.S. Patil, Effect of phase-transfer catalysts on the interfacial tension of water/toluene system, Can. J. Chem. Eng. 71 (1993) 802–804.
[11] J. Saien, S. Akbari, Interfacial tension of toluene + water + sodium dodecyl sulfate from (20 to 50) °C and pH between 4 and 9, J. Chem. Eng. Data 51 (2006) 1832–1835.
[12] S. Gao, K. Moran, Z. Xu, J. Masliyah, Role of bitumen components in stabilizing water-in-diluted oil emulsions, Energy fuels. 23 (2009) 2606–2612.
[13] S. Zeppieri, J. Rodríguez, A.L. López de Ramos, Interfacial tension of alkane + water systems, J. Chem. Eng. Data 46 (2001) 1086–1088.
[14] G. Wiegand, E.U. Franck, Interfacial tension between water and non-polar fluids up to 473 K and 2800 bar, Ber. Bunsen-Ges. Phys. Chem. 98 (1994) 809–817.
[15] R. Aveyard, D.A. Haydon, Thermodynamic properties of aliphatic hydrocarbon/water interfaces, Trans. Faraday Soc. 61 (1965) 2255–2261.
[16] A.S. Michaels, E.A. Hauser, Interfacial tension at elevated pressure and temperature. II. Interfacial properties of hydrocarbon–water systems, J. Phys. Chem. 55 (1951) 408–421.
[17] S.S. Susnar, H.A. Hamza, A.W. Neumann, Pressure dependence of interfacial tension of hydrocarbon—water systems using axisymmetric drop shape analysis, Colloids Surf. A 89 (1994) 169–180.
[18] A. Georgiadis, G. Maitland, J.P.M. Trusler, A. Bismarck, Interfacial tension measurements of the (H_2O + *n*-decane + CO_2) ternary system at elevated pressures and temperatures, J. Chem. Eng. Data 56 (2011) 4900–4908.
[19] N. Matubayasi, K. Motomura, S. Kaneshina, M. Nakamura, R. Matuura, Effect of pressure on interfacial tension between oil and water, Bull. Chem. Soc. Jpn. 50 (1977) 523–524.
[20] F.G. McCaffery, Measurement of interfacial tensions and contact angles at high temperature and pressure, J. Can. Pet. Technol. 11 (1972) 26–32.
[21] H.Y. Jennings, The effect of temperature and pressure on the interfacial tension of benzene-water and normal decane-water, J. Colloid Interface Sci. 24 (1967) 323–329.
[22] P. Linse, Monte Carlo simulation of liquid–liquid benzene–water interface, J. Chem. Phys. 86 (1987) 4177–4187.
[23] F. Biscay, A. Ghoufi, V. Lachet, P. Malfreyt, Monte Carlo calculation of the methane-water interfacial tension at high pressures, J. Chem. Phys. 131 (2009) 124707.
[24] J.P. Nicolas, N.R. de Souza, Molecular dynamics study of the n-hexane–water interface: towards a better understanding of the liquid–liquid interfacial broadening, J. Chem. Phys. 120 (2004) 2464–2469.
[25] S.S. Jang, S.T. Lin, P.K. Maiti, M. Blanco, W.A. Goddard, P. Shuler, Y.C. Tang, Molecular dynamics study of a surfactant-mediated decane–water interface: effect of molecular architecture of alkyl benzene sulfonate, J. Phys. Chem. B 108 (2004) 12130–12140.
[26] A.R. van Buuren, S.J. Marrink, H.J.C. Berendsen, A molecular dynamics study of the decane/water interface, J. Phys. Chem. 97 (1993) 9206–9212.
[27] J.L. Rivera, C. McCabe, P.T. Cummings, Molecular simulations of liquid-liquid interfacial properties: water–n-alkane and water-methanol–n-alkane systems, Phys. Rev. E 67 (2003) 011603.
[28] M. Kunieda, K. Nakaoka, Y.F. Liang, C.R. Miranda, A. Ueda, S. Takahashi, H. Okabe, T. Matsuoka, Self-accumulation of aromatics at the oil–water interface through weak hydrogen bonding, J. Am. Chem. Soc. 132 (2010) 18281–18286.
[29] H. Rezaei, H. Modarress, Dissipative particle dynamics (DPD) study of hydrocarbon–water interfacial tension (IFT), Chem. Phys. Lett. 620 (2015) 114–122.
[30] M. Ndao, J. Devemy, A. Ghoufi, P. Malfreyt, Coarse-Graining the liquid–liquid interfaces with the MARTINI force field: how is the interfacial tension reproduced? J. Chem. Theory Comput. 11 (2015) 3818–3828.
[31] J.C. Neyt, A. Wender, V. Lachet, A. Ghoufi, P. Malfreyt, Quantitative predictions of the interfacial tensions of liquid–liquid interfaces through atomistic and coarse grained models, J. Chem. Theory Comput. 10 (2014) 1887–1899.
[32] O. Lobanova, A. Mejía, G. Jackson, E.A. Müller, SAFT-γ force field for the simulation of molecular fluids 6: binary and ternary mixtures comprising water, carbon dioxide, and *n*-alkanes, J. Chem. Thermodyn. 93 (2016) 320–336.
[33] A. Ghoufi, P. Malfreyt, D.J. Tildesley, Computer modelling of the surface tension of the gas–liquid and liquid–liquid interface, Chem. Soc. Rev. 45 (2016) 1387–1409.
[34] J.M. Wang, R.M. Wolf, J.W. Caldwell, P.A. Kollman, D.A. Case, Development and testing of a general Amber force field, J. Comput. Chem. 25 (2004) 1157–1174.
[35] C.J. Dickson, B.D. Madej, Å.A. Skjevik, R.M. Betz, K. Teigen, I.R. Gould, R.C. Walker, Lipid14: the Amber lipid force field, J. Chem. Theory Comput. 10 (2014) 865–879.
[36] B. Jójárt, T.A. Martinek, Performance of the general amber force field in modeling aqueous POPC membrane bilayers, J. Comput. Chem. 28 (2007) 2051–2058.
[37] S.W.I. Siu, R. Vácha, P. Jungwirth, R.A. Böckmann, Biomolecular simulations of membranes: physical properties from different force fields, J. Chem. Phys. 128 (2008) 125103.
[38] S.W. Chiu, S.A. Pandit, H.L. Scott, E. Jakobsson, An improved united atom force field for simulation of mixed lipid bilayers, J. Phys. Chem. B 113 (2009) 2748–2763.
[39] D. Poger, W.F. Van Gunsteren, A.E. Mark, A new force field for simulating phosphatidylcholine bilayers, J. Comput. Chem. 31 (2010) 1117–1125.
[40] A.A. Skjevik, B.D. Madej, R.C. Walker, K. Teigen, LIPID11: a modular framework for lipid simulations using Amber, J. Phys. Chem. B 116 (2012) 11124–11136.
[41] S.W.I. Siu, K. Pluhackova, R.A. Bockmann, Optimization of the OPLS-AA force field for long hydrocarbons, J. Chem. Theory Comput. 8 (2012) 1459–1470.
[42] O.A. Moultos, I.N. Tsimpanogiannis, A.Z. Panagiotopoulos, J.P.M. Trusler, I.G. Economou, Atomistic molecular dynamics simulations of carbon dioxide diffusivity in n-hexane, n-decane, n-hexadecane, cyclohexane, and squalane, J. Phys. Chem. B 120 (2016) 12890–12900.
[43] W.D. Cornell, P. Cieplak, C.I. Bayly, I.R. Gould, K.M. Merz, D.M. Ferguson, D.C. Spellmeyer, T. Fox, J.W. Caldwell, P.A. Kollman, A second generation force field for the simulation of proteins, nucleic acids, and organic molecules, J. Am. Chem. Soc. 118 (1996) 2309.
[44] V. Kumar, K.S. Rane, S. Wierzchowski, M. Shaik, J.R. Errington, Evaluation of the performance of GAFF and CGenFF in the prediction of liquid-vapor saturation properties of naphthalene derivatives, Ind. Eng. Chem. Res. 53 (2014) 16072–16081.
[45] C. Caleman, P.J. van Maaren, M.Y. Hong, J.S. Hub, L.T. Costa, D. van der Spoel, Force field benchmark of organic liquids: density, enthalpy of vaporization, heat capacities, surface tension, compressibility, expansion coefficient and dielectric constant, J. Chem. Theory Comput. 8 (2012) 61–74.
[46] A.D. Becke, Density-functional thermochemistry. III. The role of exact exchange, J. Chem. Phys. 98 (1993) 5648–5652.
[47] P.J. Stephens, F.J. Devlin, C.F. Chabalowski, M.J. Frisch, *Ab Initio* calculation of vibrational absorption and circular dichroism spectra using Density Functional force fields, J. Phys. Chem. 98 (1994) 11623–11627.
[48] W.J. Hehre, R. Ditchfield, J.A. Pople, Self—consistent molecular orbital methods. XII. Further extensions of Gaussian—type basis sets for use in molecular orbital studies of organic molecules, J. Chem. Phys. 56 (1972)

2257–2261.
[49] M.J. Frisch, G.W. Trucks, H.B. Schlegel, G.E. Scuseria, M.A. Robb, J.R. Cheeseman, G. Scalmani, V. Barone, B. Mennucci, G.A. Petersson, H. Nakatsuji, M. Caricato, X. Li, H.P. Hratchian, A.F. Izmaylov, J. Bloino, G. Zheng, J.L. Sonnenberg, M. Hada, M. Ehara, K. Toyota, R. Fukuda, J. Hasegawa, M. Ishida, T. Nakajima, Y. Honda, O. Kitao, H. Nakai, T. Vreven, J.A. Montgomery Jr., J.E. Peralta, F. Ogliaro, M.J. Bearpark, J. Heyd, E.N. Brothers, K.N. Kudin, V.N. Staroverov, R. Kobayashi, J. Normand, K. Raghavachari, A.P. Rendell, J.C. Burant, S.S. Iyengar, J. Tomasi, M. Cossi, N. Rega, N.J. Millam, M. Klene, J.E. Knox, J.B. Cross, V. Bakken, C. Adamo, J. Jaramillo, R. Gomperts, R.E. Stratmann, O. Yazyev, A.J. Austin, R. Cammi, C. Pomelli, J.W. Ochterski, R.L. Martin, K. Morokuma, V.G. Zakrzewski, G.A. Voth, P. Salvador, J.J. Dannenberg, S. Dapprich, A.D. Daniels, Ö. Farkas, J.B. Foresman, J.V. Ortiz, J. Cioslowski, D.J. Fox, Gaussian 09, Gaussian, Inc., Wallingford, CT, USA, 2009.
[50] B.H. Besler, K.M. Merz, P.A. Kollman, Atomic charges derived from semi-empirical methods, J. Comput. Chem. 11 (1990) 431–439.
[51] U.C. Singh, P.A. Kollman, An approach to computing electrostatic charges for molecules, J. Comput. Chem. 5 (1984) 129–145.
[52] C.I. Bayly, P. Cieplak, W.D. Cornell, P.A. Kollman, A well-behaved electrostatic potential based method using charge restraints for deriving atomic charges: the RESP model, J. Phys. Chem. 97 (1993) 10269–10280.
[53] J.M. Wang, W. Wang, P.A. Kollman, D.A. Case, Automatic atom type and bond type perception in molecular mechanical calculations, J. Mol. Graph. Model. 25 (2006) 247–260.
[54] D.A. Case, T.A. Darden, T.E.I. Cheatham, C.L. Simmerling, J. Wang, R.E. Duke, R. Luo, R.C. Walker, W. Zhang, K.M. Merz, B. Roberts, S. Hayik, A. Roitberg, G. Seabra, J. Swails, A.W. Goetz, I. Kolossváry, K.F. Wong, F. Paesani, J. Vanicek, R.M. Wolf, J. Liu, X. Wu, S.R. Brozell, T. Steinbrecher, H. Gohlke, Q. Cai, X. Ye, J. Wang, M.-J. Hsieh, G. Cui, D.R. Roe, D.H. Mathews, M.G. Seetin, R. Salomon-Ferrer, C. Sagui, V. Babin, T. Luchko, S. Gusarov, A. Kovalenko, P.A. Kollman, AMBER12, University of California, San Francisco, 2012.
[55] J.L.F. Abascal, C. Vega, A general purpose model for the condensed phases of water: TIP4P/2005, J. Chem. Phys. 123 (2005) 234505.
[56] W.L. Jorgensen, J. Chandrasekhar, J.D. Madura, R.W. Impey, M.L. Klein, Comparison of simple potential functions for simulating liquid water, J. Chem. Phys. 79 (1983) 926–935.
[57] H.J.C. Berendsen, J.R. Grigera, T.P. Straatsma, The missing term in effective pair potentials, J. Phys. Chem. 91 (1987) 6269–6271.
[58] C. Vega, J.L. Abascal, M.M. Conde, J.L. Aragones, What ice can teach us about water interactions: a critical comparison of the performance of different water models, Faraday Discuss. 141 (2009) 251–276.
[59] C. Vega, E. de Miguel, Surface tension of the most popular models of water by using the test-area simulation method, J. Chem. Phys. 126 (2007) 154707.
[60] H. Jiang, O.A. Moultos, I.G. Economou, A.Z. Panagiotopoulos, Hydrogen-bonding polarizable intermolecular potential model for water, J. Phys. Chem. B 120 (2016) 12358–12370.
[61] C. Vega, J.L.F. Abascal, Simulating water with rigid non-polarizable models: a general perspective, Phys. Chem. Chem. Phys. 13 (2011) 19663–19688.
[62] F.T. Smith, Atomic distortion and the combining rule for repulsive potentials, Phys. Rev. A 5 (1972) 1708–1713.
[63] A.J. Haslam, A. Galindo, G. Jackson, Prediction of binary intermolecular potential parameters for use in modelling fluid mixtures, Fluid Phase Equilib. 266 (2008) 105–128.
[64] V.K. Michalis, O.A. Moultos, I.N. Tsimpanogiannis, I.G. Economou, Molecular dynamics simulations of the diffusion coefficients of light n-alkanes in water over a wide range of temperature and pressure, Fluid Phase Equilib. 407 (2016) 236–242.
[65] O.A. Moultos, I.N. Tsimpanogiannis, A.Z. Panagiotopoulos, I.G. Economou, Atomistic molecular dynamics simulations of CO_2 diffusivity in H_2O for a wide range of temperatures and pressures, J. Phys. Chem. B 118 (2014) 5532–5541.
[66] O.A. Moultos, G.A. Orozco, I.N. Tsimpanogiannis, A.Z. Panagiotopoulos, I.G. Economou, Atomistic molecular dynamics simulations of H_2O diffusivity in liquid and supercritical CO_2, Mol. Phys. 113 (2015) 3383.
[67] G.A. Orozco, O.A. Moultos, H. Jiang, I.G. Economou, A.Z. Panagiotopoulos, Molecular simulation of thermodynamic and transport properties for the H_2O+NaCl system, J. Chem. Phys. 141 (2014) 234507.
[68] M. Rouha, I. Nezbeda, Second virial coefficients: a route to combining rules? Mol. Phys. (2016) 1–9.
[69] I. Nezbeda, F. Moucka, W.R. Smith, Recent progress in molecular simulation of aqueous electrolytes: force fields, chemical potentials and solubility, Mol. Phys. 114 (2016) 1665–1690.
[70] D. Ballal, P. Venkataraman, W.A. Fouad, K.R. Cox, W.G. Chapman, Isolating the non-polar contributions to the intermolecular potential for water-alkane interactions, J. Chem. Phys. 141 (2014) 064905.
[71] J.G. McDaniel, A. Yethiraj, Comment on Isolating the non-polar contributions to the intermolecular potential for water-alkane interactions, J. Chem. Phys. 141 (2014) 064905. J. Chem. Phys., 144 (2016) 137101.
[72] D. Asthagiri, D. Ballal, P. Venkataraman, W.A. Fouad, K.R. Cox, W.G. Chapman, Response to "Comment on 'Isolating the non-polar contributions to the intermolecular potential for water-alkane interactions'", J. Chem. Phys. 144 (2016) 137101. J. Chem. Phys., 144 (2016) 137102.
[73] Scienomics, MAPS Platform, Paris, France, 2015.
[74] J. Ramos, L.D. Peristeras, D.N. Theodorou, Monte Carlo simulation of short chain branched polyolefins in the molten state, Macromolecules 40 (2007) 9640–9650.
[75] A.W. Sousa da Silva, W.F. Vranken, ACPYPE - AnteChamber PYthon Parser interfacE, BMC Res. Notes 5 (2012) 367.
[76] K.D. Papavasileiou, O.A. Moultos, I.G. Economou, GROMACS IFT input topologies and conformations used in the research article entitled: predictions of water/oil interfacial tension at elevated temperatures and pressures: a molecular dynamics simulation study with biomolecular force fields, Mendeley Data (2017) v2, 10.17632/y58ffdwkyt.2.
[77] E. Lindahl, B. Hess, D. van der Spoel, GROMACS 3.0: a package for molecular simulation and trajectory analysis, J. Mol. Model 7 (2001) 306–317.
[78] D. Van Der Spoel, E. Lindahl, B. Hess, G. Groenhof, A.E. Mark, H.J.C. Berendsen, GROMACS: fast, flexible, and free, J. Comput. Chem. 26 (2005) 1701–1718.
[79] H.J.C. Berendsen, D. van der Spoel, R. van Drunen, GROMACS: a message-passing parallel molecular dynamics implementation, Comput. Phys. Commun. 91 (1995) 43–56.
[80] H. Bekker, H.J.C. Berendsen, E.J. Dijkstra, S. Achterop, R. Vondrumen, D. Vanderspoel, A. Sijbers, H. Keegstra, B. Reitsma, M.K.R. Renardus, GROMACS - a parallel computer for molecular-dynamics simulations, in: R.A. DeGroot, J. Nadrchal (Eds.), 4th International Conference on Computational Physics (PC 92), World Scientific Publishing, 1993.
[81] B. Hess, C. Kutzner, D. van der Spoel, E. Lindahl, GROMACS 4: algorithms for highly efficient, load-balanced, and scalable molecular simulation, J. Chem. Theory Comput. 4 (2008) 435–447.
[82] H.J.C. Berendsen, J.P.M. Postma, W.F. van Gunsteren, A. DiNola, J.R. Haak, Molecular dynamics with coupling to an external bath, J. Chem. Phys. 81 (1984) 3684–3690.
[83] T. Darden, D. York, L. Pedersen, Particle mesh Ewald: an N·log(N) method for Ewald sums in large systems, J. Chem. Phys. 98 (1993) 10089–10092.
[84] R. Salomon-Ferrer, A.W. Götz, D. Poole, S. Le Grand, R.C. Walker, Routine microsecond molecular dynamics simulations with AMBER on GPUs. 2, Explic. solvent Part. Mesh Ewald 9 (2013) 3878–3888.
[85] B. Hess, H. Bekker, H.J.C. Berendsen, J.G.E.M. Fraaije, LINCS: a linear constraint solver for molecular simulations, J. Chem. Theory Comput. 18 (1997) 1463–1472.
[86] J.S. Rowlinson, B. Widom, Molecular Theory of Capillarity, Clarendon Press, Oxford, 1982.
[87] M. Jorge, M.N.D.S. Cordeiro, Molecular dynamics study of the interface between water and 2-nitrophenyl octyl ether, J. Phys. Chem. B 112 (2008) 2415–2429.
[88] S.E. Feller, R.W. Pastor, Constant surface tension simulations of lipid bilayers: the sensitivity of surface areas and compressibilities, J. Chem. Phys. 111 (1999) 1281–1287.
[89] W.G. Hoover, Canonical dynamics: equilibrium phase-space distributions, Phys. Rev. A 31 (1985) 1695–1697.
[90] C.L. Wennberg, T. Murtola, B. Hess, E. Lindahl, Lennard-Jones lattice summation in bilayer simulations has critical effects on surface tension and lipid properties, J. Chem. Theory Comput. 9 (2013) 3527–3537.
[91] L. Lundberg, O. Edholm, Dispersion corrections to the surface tension at planar surfaces, J. Chem. Theory Comput. 12 (2016) 4025–4032.
[92] N.M. Fischer, P.J. van Maaren, J.C. Ditz, A. Yildirim, D. van der Spoel, Properties of organic liquids when simulated with long-range Lennard-Jones interactions, J. Chem. Theory Comput. 11 (2015) 2938–2944.
[93] E.W. Lemmon, M.O. McLinden, D.G. Friend, Thermophysical properties of fluid systems, in: P.J. Linstrom, W.G. Mallard (Eds.), NIST Chemistry WebBook, NIST Standard Reference Database Number 69, National Institute of Standards and Technology, Gaithersburg MD, 20899,10.18434/T4D303, retrieved March 14, 2017.